TÜBİTAK

Turkish Journal of Chemistry

http://journals.tubitak.gov.tr/chem/

Research Article

Turk J Chem
(2020) 44: 1574-1586

doi:10.3906/kim-2007-40

Design of novel substituted phthalocyanines; synthesis and fluorescence, DFT, photovoltaic properties

Mehmet Salih AĞIRTAŞ[1,*], Derya GÜNGÖRDÜ SOLĞUN[1], Ümit YILDIKO[2], Abdullah ÖZKARTAL[3]

[1]Department of Chemistry, Faculty of Science, Van Yüzüncü Yıl University, Van, Turkey
[2]Architecture and Engineering Faculty, Department of Bioengineering, Kafkas University, Kars, Turkey
[3]Department of Physics, Faculty of Science, Van Yüzüncü Yıl University, Van, Turkey

Received: 21.07.2020 • **Accepted/Published Online:** 25.09.2020 • **Final Version:** 16.12.2020

Abstract: The 4-(2-[3,4-dimethoxyphenoxy] phenoxy) phthalonitrile was synthesized as the starting material of new syntheses. Zinc, copper, and cobalt phthalocyanines were achieved by reaction of starting compound with $Zn(CH_3COO)_2$, $CuCl_2$, and $CoCl_2$ metal salts. Basic spectroscopic methods such as nuclear magnetic resonance electronic absorption, mass and infrared spectrometry were used in the structural characterization of the compounds. Absorption, excitation, and emission measurements of the fluorescence zinc phthalocyanine compound were also investigated in THF. Then, structural, energy, and electronic properties for synthesized metallophthalocyanines were determined by quantum chemical calculations, including the DFT method. The bandgap of HOMO and LUMO was determined to be chemically active. Global reactivity (I, A, η, s, μ, χ, ω) and nonlinear properties were studied. In addition, molecular electrostatic potential (MEP) maps were drawn to identify potential reactive regions of metallophthalocyanine (M-Pc) compounds. Photovoltaic performances of phthalocyanine compounds for dye sensitive solar cells were investigated. The solar conversion efficiency of DSSC based on copper, zinc, and cobalt phthalocyanine compounds was 1.69%, 1.35%, and 1.54%, respectively. The compounds have good solubility and show nonlinear optical properties. Zinc phthalocyanine gave fluorescence emission.

Key words: Fluorescence, phthalocyanine, synthesis, DFT, photovoltaic

1. Introduction

There are many reasons that make phthalocyanine compounds interesting. One of them that stands out is the 18 π electron richness related to the chemical structure [1]. This electronic structure adds interesting properties to the compound by providing delocalization [2]. In this context, solar cells [3,4], nonlinear optics [5], chemical sensors [6], liquid crystals [7], laser dyes [8], photocatalytic [9], catalytic [10], photovoltaic [11], photochromic [12], and photodynamic therapy (PDT) [13,14] are being investigated extensively for obtaining photosensitive agents. Despite these wide uses, there are problems with phthalocyanines that need to be investigated. One of these problems is that these compounds do not dissolve to the desired level in water and most organic solvents [15]. To solve this problem, the most effective method of improving resolution is the chemical bonding of substituted groups suitable for peripheral or axial positions. When the solubility problem is overcome, these compounds can potentially be used in many fields (such as photosensor agents in PDT) [16]. The focus of research to solve this problem is the use of new original substituent groups. Recently, researchers have been focusing on the use of phthalocyanine compounds in dye-sensitive solar cells. Studies in this field are seen as an alternative for clean energy and a clean environment. Compounds that provide high power conversion efficiency are regarded as an effective candidate for dye-sensitive solar cells [16]. Therefore, the synthesis of new types of phthalocyanine complexes that are sensitive to dye is necessary [16,17]. It helps to obtain different alternatives for clean and renewable energy with the synthesis of suitable compounds. Also, phthalocyanines have lower economic costs than sensitizers such as ruthenium used for a dye-sensitized solar cell.

Herein, fluorescence, aggregation, photovoltaic performance properties, and synthesis of tetra 3,4-dimethoxyphenethoxyphenoxy phthalocyaninato complexes were reported. In addition to the experimental studies of synthesized metal complex molecules, geometry, conformational stability, and electronic properties have been investigated. For this purpose, in this study, we defined the molecular structure, nonlinear optic (NLO) analysis, molecular electrostatic potential (MEP) maps, and molecular surface properties. Quantum chemical studies were calculated according to a 6-311

* Correspondence: salihagirtas@hotmail.com

G basis set in the ground state and DFT/B3LYP levels. Furthermore, HOMO and LUMO energies, total energy, ΔE (LUMO-HOMO) energy gap, and global reactivity descriptors (I, A, η, s, μ, χ, ω) were calculated. For the phthalocyanines used here, the high power conversion efficiency was found at a reasonable performance level.

2. Experimental section

All information about the used equipment, materials, synthesis, theoretical analysis, and photovoltaic experiments is given in the Supplementary Information.

3. Results and discussion

3.1. Synthesis and characterization

The synthesis reactions of the 4-(2-[3,4-dimethoxyphenethoxy] phenoxy) phthalonitrile (**3**) and zinc (II), cobalt (II), and copper (II) phthalocyanines are shown in Scheme 1. Synthesis of 4-(2-[3,4-dimethoxyphenoxy] phenoxy) phthalonitrile (**3**) was carried out by nitro groups of nitrophenol and 4-nitrophthalonitrile compounds displacement reaction with 2-(3,4-dimethoxyphenyl) ethanol. Literature methods with minor modifications were used in the synthesis of the phthalonitrile derivative [18]. The synthesis of 4-(2-[3,4-dimethoxyphenoxy] phenoxy) phthalonitrile was carried out in a basic medium. Dry K_2CO_3 was used to make the reaction medium basic. K_2CO_3 is widely used for this type of reaction [19,20]. The reaction was monitored and followed by thin-layer chromatography. The terminated reaction was precipitated with water and isolated. This product was used as the starting compound in the preparation of zinc, cobalt, and copper phthalocyanines. Phthalocyanine complexes synthesized using this starting material dissolve easily in CH_2Cl_2, $CHCl_3$, THF, DMF, and DMSO. Phthalocyanine complexes, which are easily soluble in solvents, can be used more in applications. One of the obstacles in applications of phthalocyanine compounds is that they are poorly soluble. To solve this problem, axial, peripheral, and nonperipheral groups are added to the phthalocyanine structure [15,21]. If the groups mentioned for solubility also prevent aggregation, they provide an advantage for applications.

The phthalocyanine complexes (**4**–**6**) were obtained by the reaction of the template cyclotetramerization of 4-(2-[3,4-dimethoxyphenethoxy] phenoxy) phthalonitrile (**3**) with metal salts ($Zn[CH_3COO]_2$, $CuCl_2$, and $CoCl_2$). The characterization of these compounds was carried out with the help of mass, FT-IR, ^{13}C-NMR, ^{1}H-NMR, and UV-Vis spectra.

As expected from the ^{1}H-NMR spectrum for compound **3**, aromatic protons were observed around 8.12–6.90 ppm. It was determined that aliphatic protons of this compound appeared at 4.34, 3.72, 3.70, 3.31, and 2.95 ppm.

In ^{13}C NMR spectrum of phthalonitrile **3** at 162.27, 160.71, 149.96, and 147.96 C=O, at 136.77–136.17 and 130.40–120.55 ppm C=C and at 116.72–116.67 ppm C≡N, at 70.13 ppm CH_2 and at 55.99–55.92 ppm CH_3 peaks were observed. These data support the expected structure. The ^{1}H and ^{13}C-NMR spectra of compound **3** are shown in Figures S1 and S2. The ^{1}H-NMR spectrum in the DMSO solvent of compound **4** also supports the construct as expected. Aromatic protons are observed as approximately 9.22, 8.81–6.85 ppm, while aliphatic protons appear at 4.73, 3.76, 3.70, 3.41, 3.36, 3.31, 3.25, 2.48, and 1.34 ppm. This phthalocyanine compound is compatible with the expected structure, except for minor chemical shifts relative to the starting material. Based on the literature information on compounds **5** and **6**, ^{1}H-NMR measurements were not made. Generally, the types of phthalocyanine complexes carrying the paramagnetic metal atom are excluded from the ^{1}H-NMR spectra [22,23].

Vibration bands of functional groups were observed in FT-IR spectral measurements as expected; 3080 (Ar–CH), 2949–2835 (CH_3), 2231 (C≡N), 1600–1517 (C=C), 1249 cm^{-1} (Ar–O–Ar) confirms the structure of the synthesized phthalonitrile. After the conversion of 4-(2-[3,4-dimethoxyphenethoxy] phenoxy) phthalonitrile **3** into phthalocyanines **4**–**6**, the sharp peak for the (C≡N) vibrations disappeared. The IR spectra of compound **4** displayed aromatic CH peaks at 3100 cm^{-1} (Ar–H), 2964–2835 cm^{-1} (CH_3), 1598 cm^{-1} (C=C), Ar–O–Ar peaks at 1261 cm^{-1}. The IR spectra of compound **5** displayed aromatic CH peaks at 3078 cm^{-1} (Ar–H), 2927–2831 cm^{-1} (CH_3), 1606–1514 cm^{-1} (C=C), Ar–O–Ar peaks at 1261 cm^{-1}. Similarly, The IR spectra of compound **6** displayed aromatic CH peaks at 3080 cm^{-1}(Ar–H), 2966–2879 cm^{-1} (CH_3), 1600–1514 cm^{-1} (C=C), Ar–O–Ar peaks at 1259 cm^{-1}. The IR spectrum values of these phthalocyanine compounds and starting material are consistent with similar functional groups in the literature [17,24]. These originally prepared phthalocyanine compounds, besides their high efficiency, are economically important to obtain in a short period of time. Confirmation of spectrally determined compounds with computational chemistry also helps to determine their electronic properties. Phthalocyanine compounds are researched for their rich electronic structures for many technological applications. In accordance with these purposes, it is necessary to investigate factors such as fluorescence, aggregation, and solubility.

3.2. Fluorescent spectra

In today's technology fluorescent compounds have important uses such as disease diagnosis and treatment [25]. Sensor materials such as biomarking [25], environmental indicators [26], enzyme substrates [27], cell-organelle marking [28],

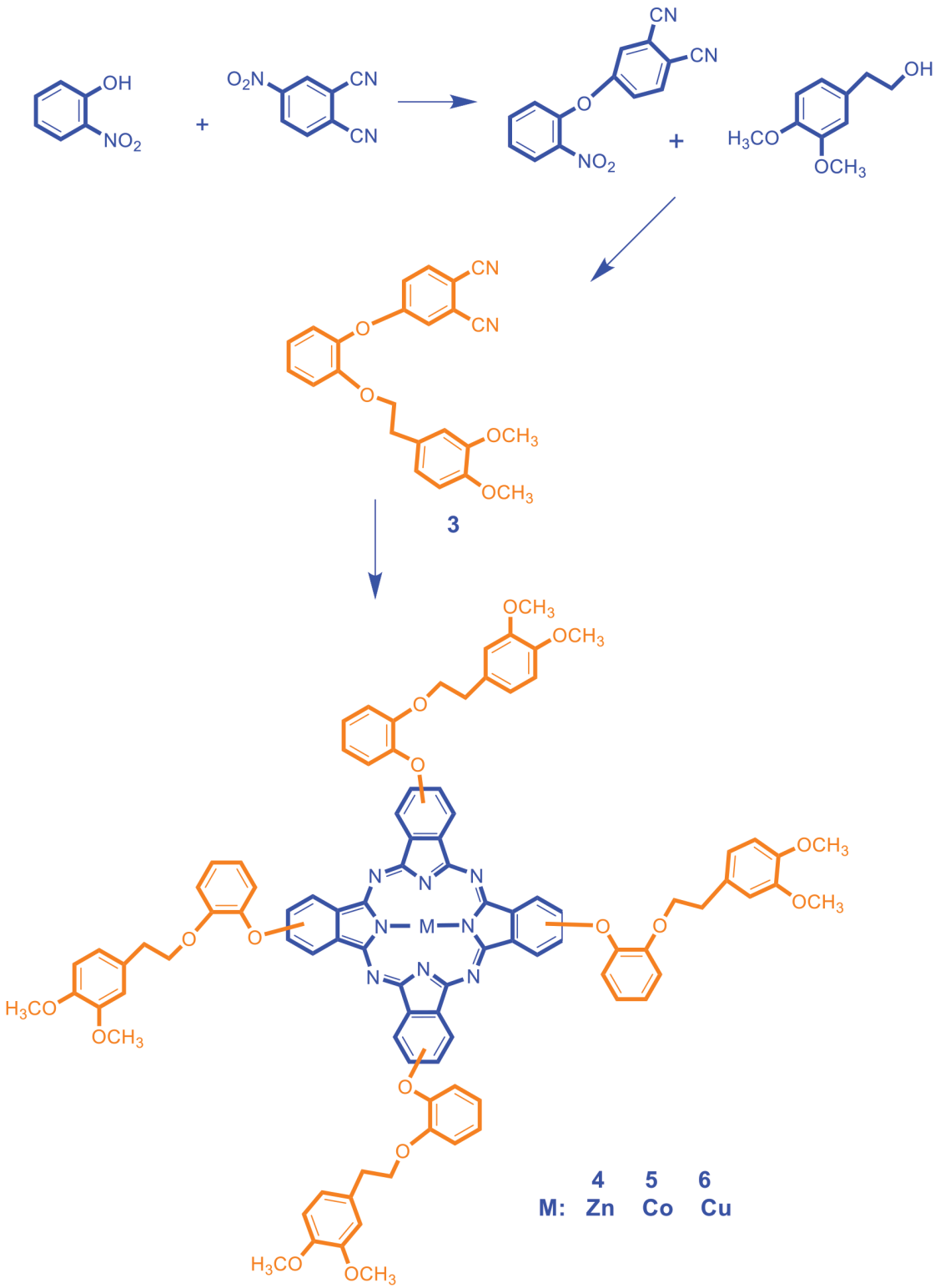

Scheme 1. Schematic representation of the synthesis of compounds (**3**–**6**).

radiation-emitting diodes [29], chemistry [30], molecules biology [30], and physics [31] have become an integral part of science. Fluorescence excitation, absorption, and emission spectra of the zinc phthalocyanine compound, which shows fluorescence from these compounds, were examined in THF solvent. Figure 1 shows these spectra. Stokes shifts observed

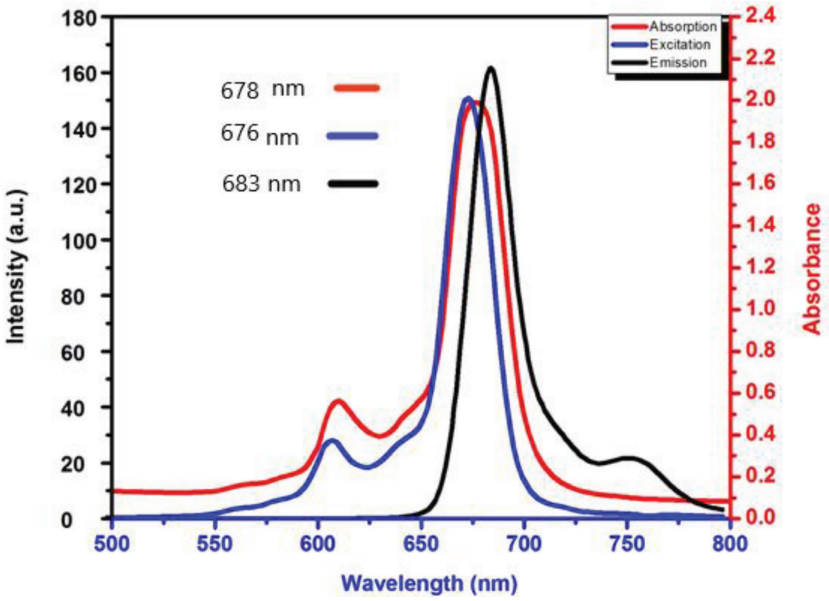

Figure 1. Emission, excitation, and absorption spectra of phthalocyanine compound **4** in THF.

for this compound fall within the appropriate range for phthalocyanines. Stokes shift values of the fluorescence zinc phthalocyanine vary depending on the solvent effect. This value was 7 nm for THF. Fluorescence excitation and emission values of phthalocyanine compound **4** values were found to be in accordance with the values in the literature [32]. The fluorescence activity of this compound allows it to find application potential in the abovementioned areas.

3.3. Electronic absorption spectra

UV-Vis spectroscopy is one of the basic devices for phthalocyanine chemistry. Phthalocyanines have specific electronic transitions thanks to 18 π electrons. These transitions are characterized by the Q band in the visible region of the spectrum, which results from π–π * electron transitions from the highest occupied molecular orbitals (HOMO) (a_{1u} and a_{2u}) to the lowest unoccupied molecular orbitals (LUMO), and occurs at about 600–700 nm. The other one is called the B band and can be seen in the 300–400 nm range due to deeper π HOMO to LUMO energy levels [33]. In this study, characteristic data for phthalocyanine compounds were obtained as expected in electronic structure. The zinc phthalocyanine complex gives a Q band in THF solvent at 676 nm and shoulder at 610 nm; similarly, the cobalt phthalocyanine complex gives a Q band at 664 nm at THF. The copper phthalocyanine complex gives a Q band in the same solvent at 676 nm and a shoulder at 610 nm. Zinc and copper phthalocyanines display B bands at 348 and 342 nm, respectively. The fact that phthalocyanines have characteristic electronic transitions in the UV visible region enables phthalocyanines to reveal other properties of UV rays such as DNA binding, DNA photocleavage, and antioxidants. This richness of electronic behavior also makes attractive the investigation of the photovoltaic behavior of these compounds.

3.4. Aggregation studies

Phthalocyanines continue to exist as many different research subjects. Essentially, there are two considerations required to overcome two important hurdles that phthalocyanine compounds face in applications. One of these is to improve the solubility of these compounds. The other is to prevent aggregation in the solvent environment. Nonaggregate phthalocyanine compounds are preferred for many applications. To investigate how these compounds behave in this solvent medium, their aggregation properties are investigated. H and J aggregates are frequently investigated in phthalocyanine chemistry. These studies reveal the behavior of the compound in the solvent [34]. The concentration-related changes of zinc, cobalt, and copper phthalocyanine compounds with electronic absorption in THF solvent are given in Figures 2 and S3–S4. In addition, the electronic absorption of these phthalocyanine compounds in different solvents to determine the effect of different solvents is given in Figures 3 and S5–S6. The concentration results in which the compounds were studied show that the compounds are not aggregated. It is known that nonaggregated phthalocyanine compounds are preferred in promising treatments such as photodynamic therapy. While phthalocyanines generally tend to aggregate in the solvent medium, the nonaggregation behavior of these compounds makes them valuable.

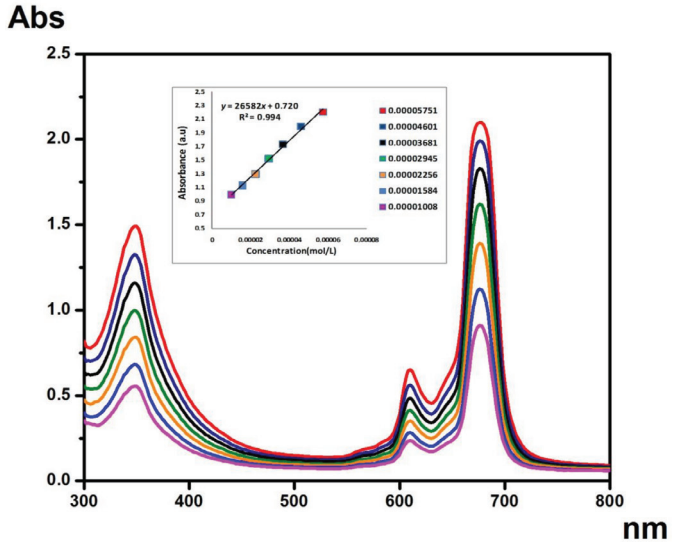

Figure 2. Electronic absorption of compound **4** in different concentrations.

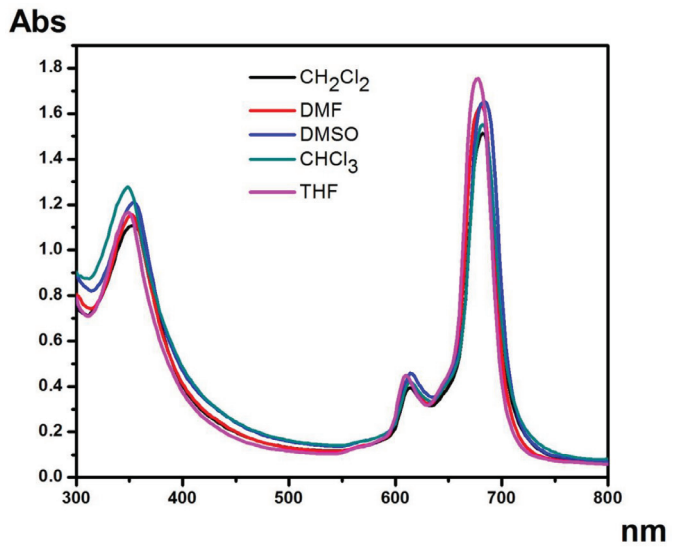

Figure 3. Electronic absorption of compound **4** in different solvents.

3.5. Geometric optimization and structural analysis

In this study, quantum chemical calculation of phthalocyanine compounds having a molecular structure with three different metal centers was performed by a DFT/B3LYP method, which contains a 6-311G basis set. The optimized structures are given in Figures 4–6. Parameters such as planar state, bond angles, and bond lengths of the phthalocyanine core were determined by optimization. In the optimization of the central atom, Zn–N5 2007, Zn–N18 2005, Cu–N5 1.973 Å, Cu–N18 1.972 Å, Co–N5 1.943 Å, and Co–N18 1.943Å were calculated. The bond lengths in the phthalocyanine core vary according to the size of the central atom. However, the values of the C4–N7 bond length are 1.331Å in Zn–Pc, 1.326 Å in Cu–Pc, and 1.336 Å in Co–Pc, and are very close to each other. The fact that the central atom is different does not have much effect on the change of other parameters. With the calculations, it has been determined that Zn41–N18–C14–C15 and C20–N19–C17–C16 atom groups have dihedral angles close to 180°. These angles show that the phthalocyanine core is planar. These parameters contribute to the determination of the molecular structure [35].

Mulliken atomic charges are orbital-based. Electronic charges in a molecule are collected according to the charge contributions from the orbitals. When determining the charge of an atom, the clouds of electrons overlapping between two

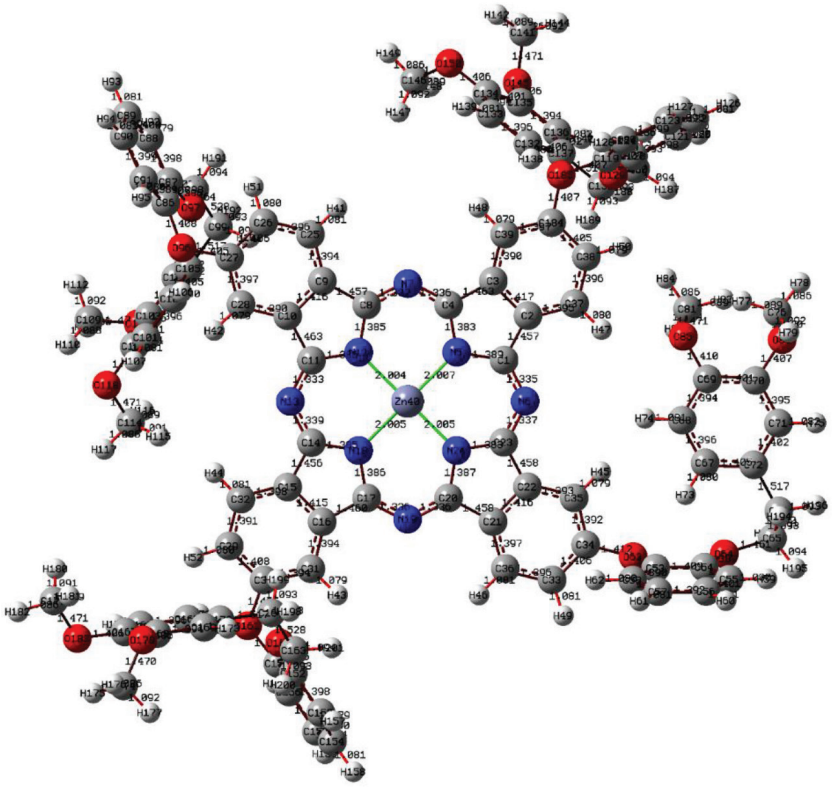

Figure 4. Optimized molecular structure of compound **4** at DFT/B3LYP/6-311G basis set.

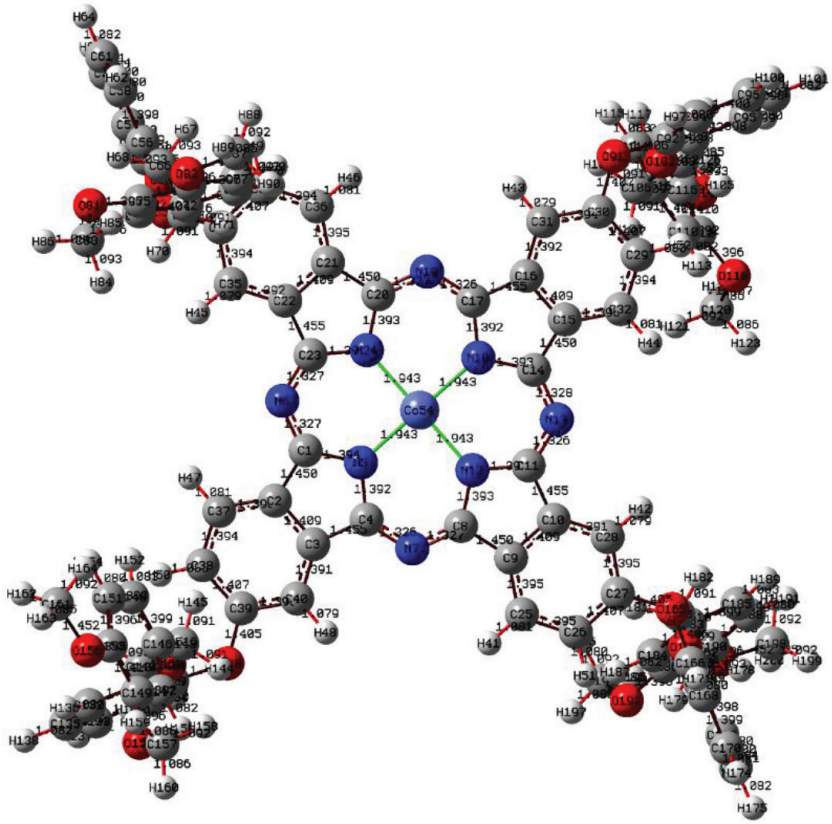

Figure 5. Optimized molecular structure of compound **5** at DFT/B3LYP/6-311G basis set.

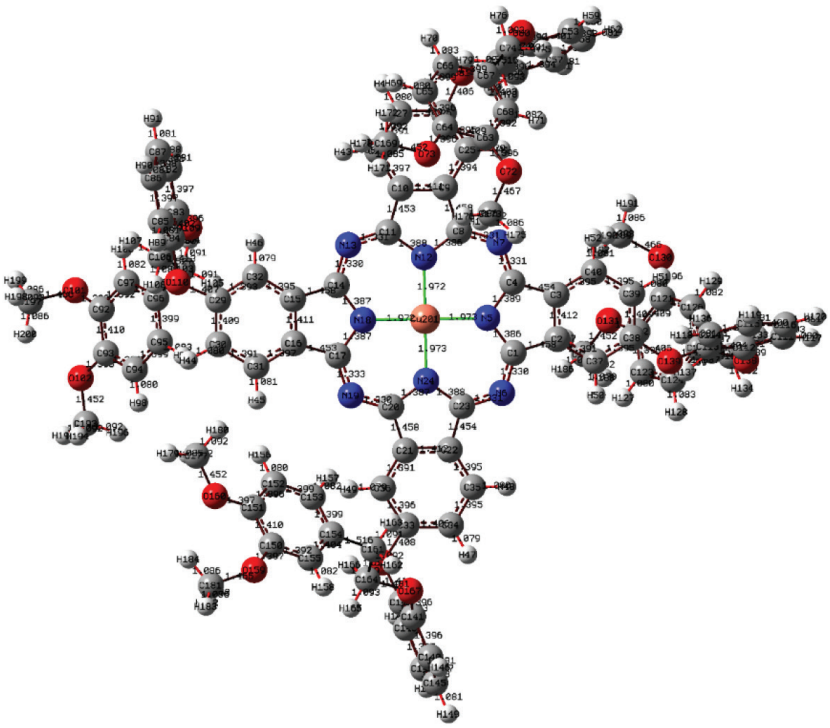

Figure 6. Optimized molecular structure of compound **6** at DFT/B3LYP/6-311G basis set.

atoms are calculated by dividing the two atoms equally [36]. Mulliken charge distribution for zinc atom, respectively; Zn41 (1.493), Cu (1.305), and Co54 (1.295), and nitrogen bound to the central atom were calculated in three phthalocyanines, N12 (–0.796), N24 (–0.795), respectively. Some C atoms in the phthalocyanine nucleus are positive and others are negative. Mulliken atomic charges are shown in Figure 7.

3.6. Energetic properties

The energy levels of HOMO-LUMO orbitals were calculated with a 6-311 basis set of DFT-B3LYP method under the Gaussian 09 package program and are shown in Figure 8 [37]. The electronic properties of the optimized compounds **4**, **5**, and **6** were visualized using the GausView 6.0 program. The results are reported here and the orbital maps of the HOMO and LUMO energies are shown in Figure 8. Molecule for Zn–Pc; E_{HOMO} = –4.8690 eV – E_{LUMO} = –2.6548 eV, calculated. Molecule for Cu–Pc; E_{HOMO} = –5.3147 eV – E_{LUMO} = –3.1364 eV, calculated. For other phthalocyanine compounds; Co–Pc E_{HOMO} = –5.1003 eV E_{LUMO} = –2.9369 eV was calculated. Table 1 shows some chemical activity parameters. The molecule with a high dipole moment has a great asymmetry in the electronic charge distribution [38]. This situation is more reactive and sensitive and can change its electronic structure and its properties under a different interaction field. For compounds to have strong electron delocalization, they must have low electronegativity, high chemical potential, and low chemical hardness [39,40]. The chemical hardness of the compounds was in the range of 1.107–1.568 eV and the chemical softness was in the range of 0.540–0.784 eV. Therefore, it is understood that the compounds have good chemical stability [41].

A dipole moment can be obtained from any standard electronic structure program. Hyperpolarizability, the nonlinear optical (NLO) property of a molecule, is quadratic electrical sensitivity per unit volume. Polarizations and hyperpolarizability characterize the return of a system in an applied electric field [38]. The dipole moment (independent of area, Debye) was calculated as Zn–Pc 4.8278, Co–Pc 4.8699, and Cu–Pc 9.2932. It is promised that these molecules will have nonlinear optical properties. The dipole moment values of zinc and cobalt phthalocyanine compounds were found close to each other. Copper phthalocyanine showed a higher dipole moment due to its electronic structure.

3.7. Molecular electrostatic potential (MEP)

MEP maps provide information about the electronic charge distribution of a molecule. The density of the electron distribution of the molecule is useful for illuminating bonds with descriptors such as polarity and electronegativity. The electronic structure and molecular reactivity of complex molecules can exhibit rich topographic properties [42].

In this study, electrophilic potential (MEP) maps of three phthalocyanine molecules were obtained. As shown in Figure 9, it is visualized with MEP maps at the DFT/B3LYP/6-311G level using the GaussView 6.0.16 software. The MEP map

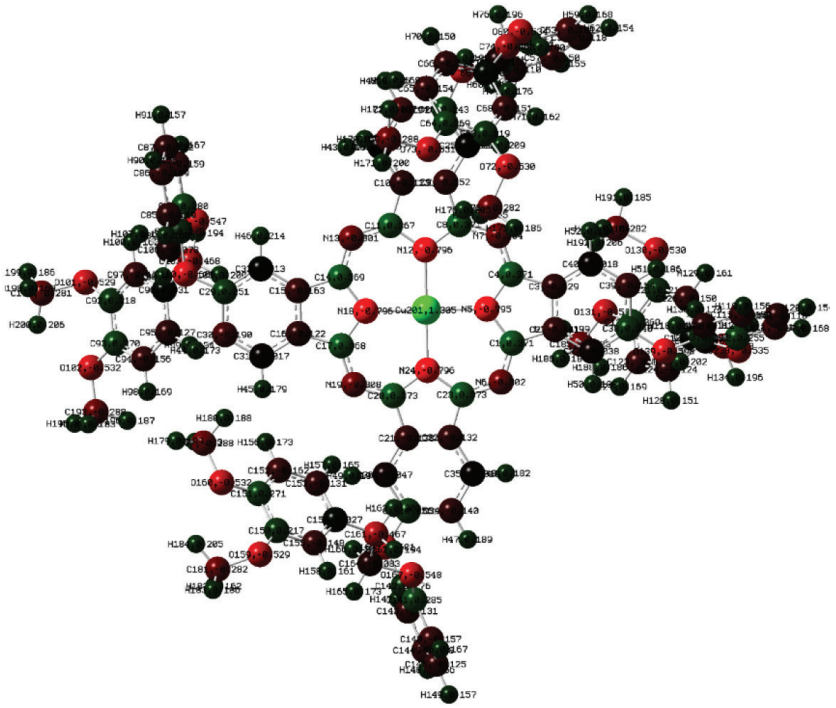

Figure 7. Mulliken atomic charges were calculated with DFT ab-initio B3LYP/6-31G (d, p).

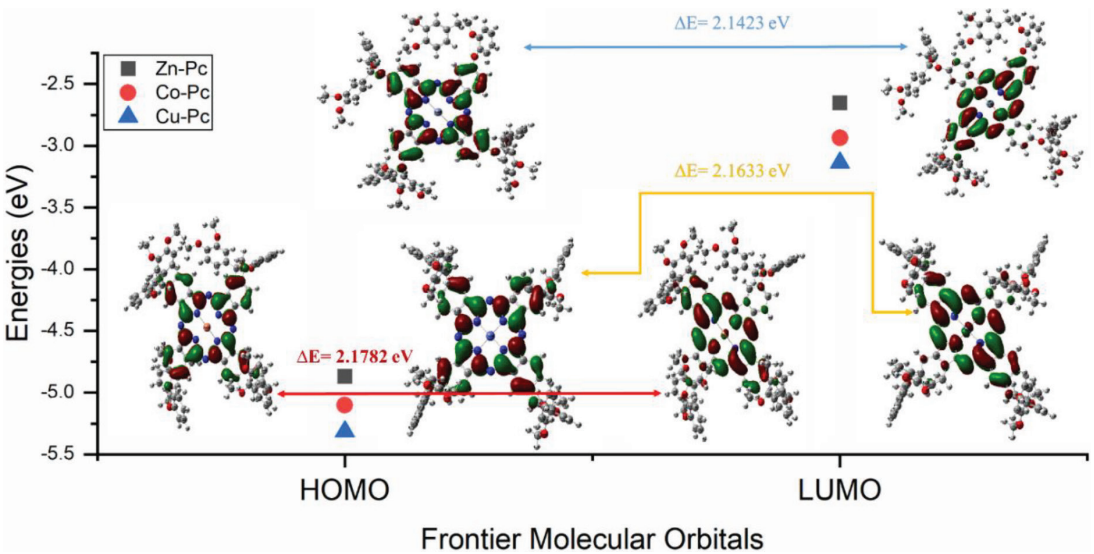

Figure 8. Frontier molecular orbitals of 3,4-dimethoxyphenethoxy) phenoxy substituted metallophthalocyanines by DFT/B3LYP with 6-311 G basis sets.

shows that the region characterized by the blue color around the Zn, Co, and Cu atoms have positive values. The red regions on the map indicate the region rich in electrons. The aromatic ring region shows an almost neutral potential, most of which is represented by a yellow–green color [43]. Contour maps of phthalocyanines confirm negative and positive potential parameters in accordance with the electrostatic potential map (ESP). The phthalocyanine core in the structures shows a delocalized structure and high stabilization with green–yellow colors.

3.8. Photovoltaic properties

The graph obtained as a result of the current voltage applied to the samples to examine the photovoltaic properties of the produced samples is given in Figure 10. J_{SC}, V_{OC}, J_{max}, and V_{max} values of the samples produced in DSSC structure, called

Table 1. E_{HOMO}, $E_{LUMO,}$ dipole moment (ρ, Debye), electronegativity (χ) and global electrophile (ω) etc. values of compounds (**4-6**).

Molecules Energy	Zn–Pc	Co–Pc	Cu–Pc
E_{LUMO}	–2.6548	–2.9369	–3.1364
E_{HOMO}	–4.8690	–5.1003	–5.3147
Energy gap (Δ)E_{HOMO}- E_{LUMO}	2.2142	2.1633	2.1782
Ionization potential ($I = -E_{HOMO}$)	4.8690	5.1003	5.3147
Electron affinity ($A = -E_{LUMO}$)	2.6548	2.9369	3.1364
Chemical hardness ($\eta = (I - A)/2$)	1.1071	1.0814	1.5682
Chemical softness ($s = 1/2\ \eta$)	0.5535	0.5408	0.7841
Chemical potential ($\mu = (I + A)/2$)	3.7619	4.0187	3.7465
Electronegativity ($\chi = (1+ A)/2$)	1.8274	1.3576	2.0683
Electrophilicity index ($\omega= \mu^2/2\ \eta$)	6.6057	7.4650	4.4753
Dipole moment (μ)	4.8278	4.8699	9.2932

compound **4**, compound **5,** and compound **6**, were obtained from the current density (J) – voltage (V) graph, Figure 10. The fill factor (FF) and the energy conversion efficiency (η) of produced samples were calculated using the following Equation 1 and Equation 2, respectively [44].

$$FF = \frac{I_{max}V_{max}}{I_{SC}V_{OC}} \tag{1}$$

$$\eta = \frac{I_{SC}V_{OC}}{P_{in}}FF \tag{2}$$

where P_{in} is the power of incident light. The values of FF and η are determined and indicated in Table 2 for all the produced samples. It can be seen that the HOMO and LUMO energy levels of the metal complexes used to form the DSSC structure are compatible with the valence band and the conduction band of TiO_2. The observed V_{oc} and I_{sc} values of each sample can be indicated with the high number of electrons that flow into a conduction band of TiO_2 from the excitement of compounds **4–6** by the absorption of the photon energy. These efficiencies of the samples show that the photovoltaic parameters of the DSSC structures are contributed by the metal complexes [45]. The results appear to be compatible with the studies in the literature [46]. Reasons such as limited reserves of fossil fuels and not being clean for the environment increase the demand for renewable energy sources. Here, the way to use solar energy economically is based on effective high power conversion efficient dye sensitive solar cells [47–50]. Dye sensitive solar cells made of phthalocyanine compounds, which are stable up to 400–500 degrees, provide the opportunity to benefit from solar energy, which is abundant, cheap, and clean. Among the reasons for the preference of phthalocyanines for this purpose, photochemical, thermal, and electrochemical stability are positive factors. Studies have reported that ruthenium polypyridyl complexes are the most common sensitizers in DSSCs, and the conversion efficiency here is about 12%. Moreover, ruthenium metal is limited for applications due to factors such as cost and environmental damage.

4. Conclusion

In this study, a new phthalonitrile derivative was synthesized. New zinc, cobalt, and copper phthalocyanine complexes were obtained from the reaction of synthesized starting material with metal salts. These compounds were characterized by general spectrophotometers. Then, fluorescence emission and absorption spectra and their properties were investigated. In addition to other properties of zinc phthalocyanine, fluorescence was characteristic. Furthermore, the compounds exhibited advantages such as nonaggregation behavior and good solubility in organic solvents. The structure of phthalocyanine molecules was examined using a 6–311 base set of DFT/B3LYP calculation method. Optimized bond lengths and angles were obtained, and it was determined that the molecular atom of the metal atom was placed planarly in the phthalocyanine nucleus. In addition, global reactivity parameters, HOMO and LUMO energy gaps that determine chemical stability, were calculated. Compounds **4–6** energy gap with soft molecular structure were calculated as close to each other as 2.2142 eV,

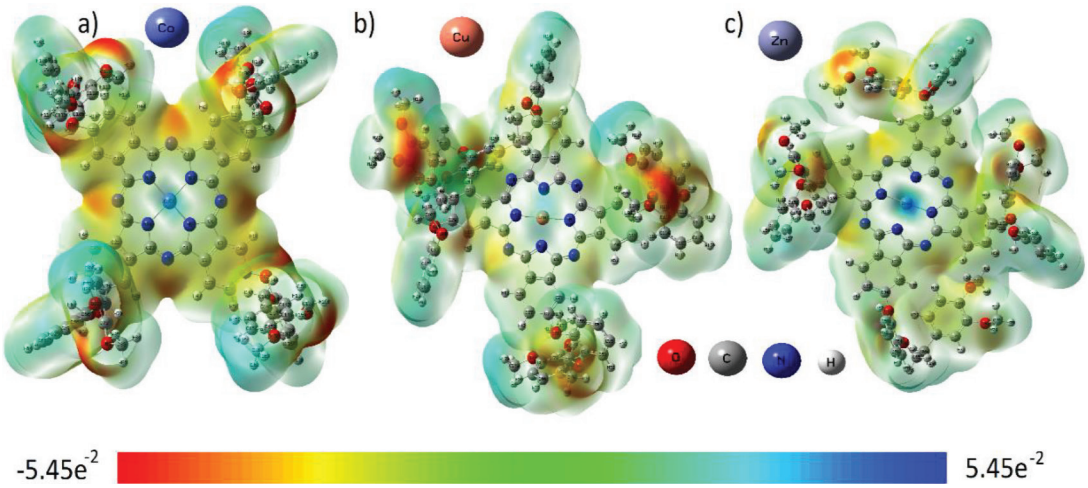

Figure 9. Molecular electrostatic potential mapped of compounds **4**–**6**.

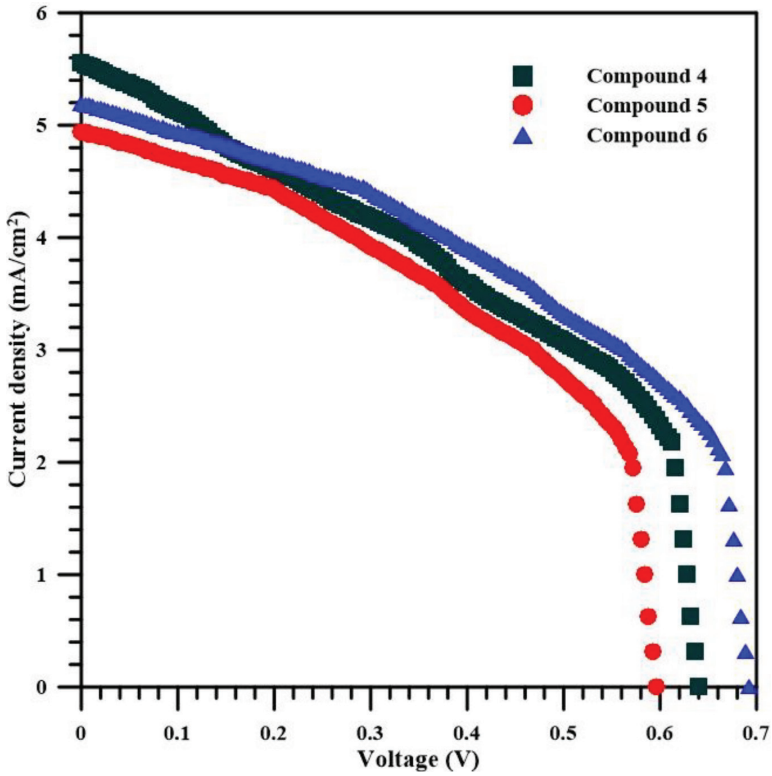

Figure 10. J-V curves of DSSCs based on phthalocyanine compounds **4**–**6**.

Table 2. The photovoltaic parameters for DSSCs based on phthalocyanine **4**-6 complexes.

Samples	J_{SC} (mA/cm²)	V_{OC} (V)	FF	H (%)
Compound **4**	5.56	0.64	0.43	1.54
Compound **5**	4.94	0.59	0.46	1.35
Compound **6**	5.20	0.69	0.47	1.69

2.1633 eV, and 2.1782 eV, respectively. Dipole moments of Zn–Pc, Co–Pc, and Cu–Pc were calculated as 4.8278, 4.8699, and 9.2932 D. The results showed that the molecules have nonlinear optical properties. The solar conversion efficiency of DSSC devices based on copper, zinc, and cobalt phthalocyanine compounds was reported as 1.69%, 1.35%, and 1.54%, respectively. The measurement results showed that the compounds can be enriched with different additives for dye-sensitive solar cell technology.

Acknowledgment
We would like to thank Van Yüzüncü Yıl University Scientific Research Projects Unit for their contribution.

References

1. Braika M, Dridia C, Ali MB, Ali A, Abbas MN et al. Investigation of structural, optical and electrical properties of a new cobalt phthalocyanine thin films with potential applications in perchlorate sensor. Synthetic Metals 2015; 209: 135-142.
2. Urbani M, Ragoussi ME, Nazeeruddin MK, Torres T. Phthalocyanines for dye-sensitized solar cells. Coordination Chemistry Reviews 2019; 381: 1-64.
3. Sfyri G, Vamshikrishna N, Kumar CV, Giribabu L, Lianos P. Synthesis and characterization of tetratriphenylamine Zn phthalocyanine as hole transporting material for perovskite solar cells. Solar Energy 2016; 140: 60-65.
4. Ali HEA, Altındal A, Altun S, Odabas Z. Highly efficient dye-sensitized solar cells based on metal-free and copper(II) phthalocyanine bearing 2-phenylphenoxy moiety. Dyes and Pigments 2016; 124: 180-187.
5. Savelyev MS, Gerasimenko AY, Podgaetskii VM, Tereshchenko SA, Selishchev SV et al. Conjugates of thermally stable phthalocyanine J-type dimers with single-walled carbon nanotubes for enhanced optical limiting applications. Optics & Laser Technology 2019; 117: 272-279.
6. Basova TV, Mikhaleva NS, Hassan AK, Kiselev VG. Thin films of fluorinated 3d-metal phthalocyanines as chemical sensors of ammonia: an optical spectroscopy study. Sensors and Actuators B: Chemical 2016; 227: 634-642.
7. Kong S, Wang X, Bai L, Song Y, Meng F. Multi-arm ionic liquid crystals formed by pyridine-mesophase and copper phthalocyanine. Journal of Molecular Liquids 2019; 288: 111012.
8. Lin KC, Doane T, Wang L, Li P, Pejic S et al. Laser spectroscopic assessment of a phthalocyanine-sensitized solar cell as a function of dye loading. Solar Energy Materials and Solar Cells 2014; 126: 155-162.
9. Yin S, Chen Y, Hu Q, Li M, Ding Y et al. In-situ preparation of iron(II) phthalocyanine modified bismuth oxybromide with enhanced visible-light photocatalytic activity and mechanism insight. Colloids and Surfaces A: Physicochemical and Engineering Aspects 2019; 575: 336-345.
10. Kheirjou S, Kheirjou R, Rezayan AH, Shakourian-Fard M, Mahmoudi Hashemi M. Selective aqueous oxidation of alcohols catalyzed by copper (II) phthalocyanine nanoparticles. Comptes Rendus Chimie 2016; 19: 314-319.
11. Ağırtaş MS. Synthesis and characterization of novel symmetrical phthalocyanines substituted with four benzo [d] [1,3] dioxol-5-ylmethoxy groups. Inorganica Chimica Acta 2007; 360: 2499-2502.
12. Hagen JP, Becerra I, Drakulich D, Dillon RO. Effect of antenna porphyrins and phthalocyanines on the photochromism of benzospiropyrans in poly(methyl methacrylate) films. Thin Solid Films 2001; 398-399: 104-109.
13. Afshari R, Ghasemi V, Shaabani S, Shaabani A, Aladaghlo Z et al. Post-modification of phthalocyanines via isocyanide-based multicomponent reactions: Highly dispersible peptidomimetic metallophthalocyanines as potent photosensitizers. Dyes and Pigments 2019; 166: 49-59.
14. Güzel E, Atsay A, Nalbantoglu S, Şaki N, Dogan AL et al. Synthesis, characterization and photodynamic activity of a new amphiphilic zinc phthalocyanine. Dyes and Pigments 2013; 97: 238-243.
15. Ağırtaş MS. Highly soluble phthalocyanines with hexadeca tert-butyl substituents. Dyes and Pigments 2008; 79: 247-251.
16. Roguin LP, Chiarante N, García Vior MC, Marino J. Zinc(II) phthalocyanines as photosensitizers for antitumor photodynamic therapy. The International Journal of Biochemistry & Cell Biology 2019; 114: 105575.
17. Sodeifian G, Saadati Ardestani N, Sajadian SA. Solubility measurement of a pigment (Phthalocyanine green) in supercritical carbon dioxide: Experimental correlations and thermodynamic modeling. Fluid Phase Equilibria 2019; 494: 61-73.
18. Sen P, Yasa Atmaca G, Erdogmus A, Demir Kanmazalp S, Dege N et al. Peripherally tetra-benzimidazole units-substituted zinc(II) phthalocyanines: Synthesis, characterization and investigation of photophysical and photochemical properties. Journal of Luminescence 2018; 194: 123-130.

19. Demirol M, Sirka L, Çalışkan E, Biryan F, Koran K et al. Synthesis and photodiode properties of chalcone substituted metallophthalocyanine. Journal of Molecular Structure 2020; 1219: 128571.

20. Cabir B, Ağırtaş MS, Duygulu E, Yuksel F. Synthesis of some metallophthalocyanines bearing 9-phenyl-9Hfluoren-9-yl) oxy functional groups and investigation of their photophysical properties. Journal of Molecular Structure 2017; 1142: 194-199.

21. Khezami K, Harmandar K, Bağda E, Bağda E, Şahin G. The new water soluble zinc(II) phthalocyanines substituted with morpholine groups- synthesis and optical properties. Journal of Photochemistry & Photobiology A: Chemistry 2020; 401: 112736.

22. Frisch GWTMJ, Schlegel HB, Scuseria GE, Robb MA, Cheeseman JR et al. Gaussian 09, Revision A.02. Wallingford, CT, USA: Gaussian, Inc., 2016.

23. Ağırtaş MS, Güven ME, Gümüş S, Özdemir S, Dündar A. Metallo and metal free phthalocyanines bearing (4-(1(4-phenoxyphenyl)-1-phenylethyl) phenol substituents: Synthesis, characterization, aggregation behavior, electronic, antioxidant and antibacterial properties. Synthetic Metals 2014; 195: 177-184.

24. Prabhaharan M, Prabakaran AR, Gunasekaran S, Srinivasan S. DFT studies on vibrational spectra, HOMO–LUMO, NBO and thermodynamic function analysis of cyanuric fluoride. Spectrochimica Acta Part A: Molecular and Biomolecular Spectroscopy 2015; 136: 494-503.

25. Attia MS, Ali K, El-Kemary M, Darwishd WM. Phthalocyanine-doped polystyrene fluorescent nanocomposite as a highly selective biosensor for quantitative determination of cancer antigen 125. Talanta 2019; 201: 185-193.

26. Wong RCH, Lo PC, Ng DKP. Stimuli responsive phthalocyanine-based fluorescent probes and photosensitizers. Coordination Chemistry Reviews 2019; 379: 30-46.

27. McRae EKS, Nevonen DE, McKennaSA, Nemykin VN. Binding and photodynamic action of the cationic zinc phthalocyanines with different types of DNA toward understanding of their cancer therapy activity. Journal of Inorganic Biochemistry 2019; 199: 110793.

28. Liu TM, Conde J, Lipinski T, Bednarkiewicz A, Huang CC. Smart NIR linear and nonlinear optical nanomaterials for cancer theranostics: prospects in photomedicine. Progress in Materials Science 2017; 88: 89-135.

29. Mantareva V, Angelov I, Kussovski V, Dimitrov R, Lapok L et al. Photodynamic efficacy of water-soluble Si(IV) and Ge(IV) phthalocyanines towards Candida albicans planktonic and biofilm cultures. European Journal of Medicinal Chemistry 2011; 46: 4430-4440.

30. Lapshina M, Ustyugov A, Baulin V, Terentiev A, Tsivadze A et al. Crown- and phosphoryl-containing metal phthalocyanines in solutions of poly(N-vinylpyrrolidone): Supramolecular organization, accumulation in cells, photo-induced generation of reactive oxygen species, and cytotoxicity. Journal of Photochemistry and Photobiology B: Biology 2020; 202: 111722.

31. Liu S, Liu C, Luan X, Yao R, Feng Y. Facile fabrication of dual emissive nanospheres via the self-assembling of CdSe@CdS and zinc phthalocyanine and their application for silver ion detection. Chemical Physics Letters 2017; 684: 321-327.

32. Singh S, Aggarwal A, Bhupathiraju NVSDK, Jovanovic IR, Landress M et al. Comparing a thioglycosylated chlorin and phthalocyanine as potentialtheranostic agents. Bioorganic & Medicinal Chemistry 2020; 28:115259.

33. Komori T, Amao Y. Dye-sensitized solar cell with the near-infrared sensitization of aluminum phthalocyanine. Journal of Porphyrins and Phthalocyanines 2003; 07: 131-136.

34. Ağırtaş MS, Cabir B, Özdemir S. Novel metal (II) phthalocyanines with 3,4,5-trimethoxybenzyloxy-substituents: synthesis, characterization, aggregation behaviour and antioxidant activity. Dyes and Pigments 2013; 96: 152-157.

35. Siddiqui N, Javed S. Quantum computational, spectroscopic investigations on ampyra (4-aminopyridine) by DFT/TD-DFT with different solvents and molecular docking studies. Journal of Molecular Structure 2021; 1224: 129021.

36. Shehab OR, Mansour AM. Exploring electronic structure, and substituent effect of some biologically active benzimidazole derivatives: experimental insights and DFT calculations. Journal of Molecular Structure 2021; 1223: 128996.

37. Kanagathara N, MaryAnjalin F, Ragavendran V, Dhanasekaran D, Usha R et al. Experimental and theoretical (DFT) investigation of crystallographic, spectroscopic and Hirshfeld surface analysis of anilinium arsenate. Journal of Molecular Structure 2021; 1223: 128965.

38. Krishna Kumar V, Sangeetha R, Barathi D, Mathammal R, Jayamani N. Vibrational assignment of the spectral data, molecular dipole moment, polarizability, first hyperpolarizability, HOMO–LUMO and thermodynamic properties of 5-nitoindan using DFT quantum chemical calculations. Spectrochimica Acta Part A: Molecular and Biomolecular Spectroscopy 2014; 118: 663-671.

39. Becker HGO. Jan Fleming, Frontier Orbitals and Organic Chemical Reactions, 1976 (book reviews). Advanced Synthesis & Catalysis 1978; 320 (5): 879-880.

40. Zhong L, Li Y, Bin H, Zhang M, Huang H et al. Ternary polymer solar cells based-on two polymer donors with similar HOMO levels and an organic acceptor with absorption extending to 850 nm. Organic Electronics 2018; 62: 89-94.

41. Barim E, Akman F. Synthesis, characterization and spectroscopic investigation of N-(2-acetylbenzofuran-3-yl)acrylamide monomer: molecular structure, HOMO–LUMO study, TD-DFT and MEP analysis. Journal of Molecular Structure 2019; 1195: 506-513.

42. Ogunsipe A, Maree D, Nyokong T. Solvent effects on the photochemical and fluorescence properties of zinc phthalocyanine derivatives. Journal of Molecular Structure 2003; 650: 131-140.

43. Mumit MA, Pal TK, Alam MA, Islam MAAAA, Paul S et al. DFT studies on vibrational and electronic spectra, HOMO–LUMO, MEP, HOMA, NBO and molecular docking analysis of benzyl-3-N-(2,4,5-trimethoxyphenylmethylene)hydrazinecarbodithioate. Journal of Molecular Structure 2020; 1220: 128715.

44. Grobosch M, Schmidt C, Kraus R, Knupfer M. Electronic properties of transition metal phthalocyanines: the impact of the central metal atom (d5–d10). Organic Electronics 2010; 11: 1483-1488.

45. Güngördü Solğun D, Horoz S, Ağırtaş MS. Synthesis of novel tetra (4-tritylphenoxy) substituted metallophthalocyanines and investigation of their aggregation, photovoltaic, solar cell properties. Inorganic And Nano-Metal Chemistry 2018; 48 (10): 508-514.

46. Ağırtaş MS, Güngördü Solğun D, Özdemir S, İzgi MS. Synthesis of tetra 3,4-dimethoxyphenethoxy peripheral substituted metallophthalocyanines and investigation of some properties. ChemistrySelect 2018; 3: 3523-3528.

47. Huang H, Cao Z, Li X, Zhang L, Liu X et al. Synthesis and photovoltaic properties of two new unsymmetricalzinc-phthalocyanine dyes. Synthetic Metals 2012; 162: 2316-2321.

48. Karaoğlan GK, Gümrükçü G, Gördük S, Can N, Gül A. Novel homoleptic, dimeric zinc(II) phthalocyanines as gate dielectric for OFET device. Synthetic Metals 2017; 230: 7-11.

49. Mathew S, Yella A, Gao P, Humphry-Baker R, Curchod BFE et al. Dye-sensitized solar cells with 13% efficiency achieved through the molecular engineering of porphyrin sensitizers. Nature Chemistry 2014; 6: 242-247.

50. Bignozzi CA, Argazzi R, Boaretto R, Busatto E, Carli S et al. The role of transition metal complexes in dye sensitized solar devices. Coordination Chemistry Reviews 2013; 257: 1472-1492.

Supplementary information

2. Experimental section

2.1. General

Hitachi U-2900 Spectrophotometer, Thermo Scientific FT-IR spectrophotometer, LC / MS (Thermo Fisher Scientific Inc., Waltham, MA, USA; TSQ-Quantum Access), Agilent 400 MHz spectrometer and Shimadzu RF-6000 spectrofluorophotometer devices were used for the structure characterization of the compounds (Agilent Technologies, Inc., Santa Clara, CA, USA; Shimadzu Corp., Kyoto, Japan). Chemicals and solvents were used commercially without purification.

2.2. 4-(2-(3,4-dimethoxyphenethoxy) phenoxy) phthalonitrile (3)

A mixture of 2-nitrophenol (0.402 g, 2.89 mmol) and 4-nitrophthalonitrile (0.500 g, 2.89 mmol) in 25 mL dimethylsulfoxide (DMSO) was stirred at room temperature under nitrogen atmosphere. After stirring for 15–20 min, 2-(3,4-dimethoxyphenyl) ethanol (0.527 g, 2.89 mmol) was added into the mixture. After stirring for 15 min, K_2CO_3 (2.2 g, 15.94 mmol) was added into the mixture over a period of 2 h. After this process, the stirring was stirred at 40 °C for a further 70 h. The reaction mixture was poured into ice water (150 mL) and precipitated.

It was filtered off, and washed with water to neutralize it. The product was dried in a vacuum oven at 80 °C. The product showed solubility in THF, DMSO, acetonitrile solvent. Yield; 0.47 g (40.61%). Mp: 132–135 °C. $C_{24}H_{20}N_2O_4$: 400.43 g/mol. HRMS (ESI); (M+H) calc. for $C_{24}H_{20}N_2O_4$: 400.43; found: 439.10 $[M+K]^+$. ^{1}H NMR (400 MHz, DMSO-d_6): (δ: ppm) 8.12, 8.01, 8.00, 7.74, 7.44, 6.90, 4.34, 3.72, 3.70, 3.31, 2.95, 2.48. ^{13}C NMR (400 MHz, DMSO-d_6): (δ: ppm) 162.27, 160.71, 149.11, 147.96, 146.67, 136.77, 136.49, 136.17, 130.40, 127.51, 126.81, 124.20,122.94,122.60,121.32,120.77,120.55, 116.72, 116.67, 116.16, 113.42, 112.36, 106.30, 70.13, 55.99, 55.92, 39.28. FT-IR spectrum (cm^{-1}): 3080(C–H aromatic),

2949, 2835, 2231(C≡N), 1600(C=C), 1517, 1467, 1442, 1301, 1249 (Ar–O–Ar), 1159, 1141, 1099, 1028, 948, 817, 752.

2.3. 2, 10, 16, 24 – Tetrakis 2-(3,4-dimethoxyphenethoxy) phenoxy phthalocyaninato) zinc (II) (4)

A mixture of 4-(2-(3,4-dimethoxyphenethoxy) phenoxy) phthalonitrile **3** (0.050 g**,** 0.0297 mmol) and $Zn(CH_3COO)_2$ (0.023 g) was powdered in a quartz crucible and heated for 5 min 230 ºC in a sealed glass tube. After reaching room temperature, the product was washed with hot and cold water, ethanol, and methanol. The product soluble in THF was collected and the solvent was removed to obtain a green solid. This compound showed solubility in dichloromethane, $CHCl_3$, THF, DMF, DMSO solvents. Yield: 56.00%. HRMS (ESI); (M+H) calc. for $C_{97}H_{83}N_8O_{16}Zn$: 1682.12; found: 1705.50 $[M+Na]^+$. UV-Vis (THF) λmax (log ε): 676 (5.32), 610(4.81), 348 (5.17). ^1H NMR (400 MHz, DMSO-d6) δ ppm: 9.22, 8.81, 7.74, 7.15, 7.03, 6.99, 6.98, 6.85, 4.73, 3.76, 3.70, 3.41, 3.36, 3.31, 3.25, 2.48, 1.34. IR spectrum (cm^{-1}): 3100, 2964, 2835, 1598, 1477, 1261, 1232, 1139, 1089, 1026, 952, 808.

2.4. 2, 10, 16, 24 – Tetrakis 2-(3,4-dimethoxyphenethoxy) phenoxy phthalocyaninato) cobalt (II) (5)

This compound was synthesized under the same conditions of phthalocyanine compound **4**, except for the metal salt ($CoCl_2$) used. Yield: 48.00%. HRMS (ESI); (M+H) calc. for $C_{97}H_{83}N_8O_{16}Co$: 1675.67; found: 1698.76 $[M+Na]^+$. UV-Vis (THF) λmax (log ε): 664 (5.25), 326 (5.20). IR spectrum (cm^{-1}): 3078, 2927, 2831, 1606, 1514, 1462, 1409, 1261, 1232, 1192, 1124, 1093, 1058, 1012, 954, 848.

2.5. 2, 10, 16, 24 – Tetrakis 2-(3,4-dimethoxyphenethoxy) phenoxy phthalocyaninato) copper (II) (6)

This compound was synthesized under the same conditions of phthalocyanine compound **4**, except for the metal salt ($CuCl_2$) used. Yield: 48.00%. HRMS (ESI); (M+H) calc. for $C_{97}H_{83}N_8O_{16}Cu$: 1680.29; found: 1703.40 $[M+Na]^+$. UV-Vis (THF) λmax (log ε): 676 (5.23), 610(4.77), 340 (5.09). IR spectrum (cm^{-1}): 3080, 2966, 2879, 1600, 1514, 1463, 1259, 1234, 1138, 1026, 927,806.

2.6. Theoretical analysis

All calculations were made using DFT calculations according to the basis set of B3LYP / 6-311G. Conformational analysis was performed with semiempirical method on PM3 set. In the next step, the values obtained with basis set 6-311 of DFT / B3LYP method were used to calculate minimum energy and bond lengths. Molecular structure, energies, NBO analysis, MESP maps of optimized geometries of M-Pc were calculated using Gaussian 09 and GaussView 6.0 package program [1-2].

2.7. The current density (J) - voltage (V) measurement

In conventional dye sensitive solar cell (DSSC) structures, fluorine doped tin oxide (FTO) coated glass substrates were used as working electrodes [3–7]. TiO_2 nanopowder, which was put into paste with polyethylene glycol (PEG300) solution, was coated on the standard cleaned substrates with the doctor blade technique. Fields covered with TiO_2 have a surface area of ~0.2 cm^2 and a thickness of ~50 μm. After coating process, the samples were annealed in a quartz furnace at 450 °C for 15 min. By using dimethylformamide (DMF) as solvent, 1 mM of phthalocyanine (Pc) solutions were dropped to the samples to obtain dye sensitive of TiO_2. For the samples expected to dry for 24 h at room temperature, the dripping process was repeated 3 times to ensure a tight covalent bond between TiO_2 and phthalocyanines. Commercially available an I^-/I_3^- electrolyte containing 50 mM iodide/tri-iodide was dropped on three samples ready to make contact and combined with platinum coated FTO glasses. The current–voltage

(I–V) measurement of samples was achieved under solar simulator with an AM1.5 filter and 100 mW/cm^2 illumination.

References

1. Frisch GWTMJ, Schlegel HB, Scuseria GE, Robb MA, Cheeseman JR et al. Gaussian 09, Revision A.02. Wallingford, CT, USA: Gaussian, Inc., 2016.
2. Chindeka F, Mashazi P, Britton J, Fomo G, Oluwole DO et al. Optimizing phthalocyanine based dye-sensitized solar cells: the role of reduced graphene oxide. Synthetic Metals 2018; 246: 236-245.
3. O'Regan B, Grätzel M. A low-cost, high-efficiency solar cell based on dye-sensitized colloidal TiO_2 films. Nature 1991; 353: 737-740.
4. Komori T, Amao Y. Dye-sensitized solar cell with the near-infrared sensitization of aluminum phthlocyanine. Journal of Porphyrins and Phthlocyanines 2003; 7: 131-136.
5. Yan X, Fan H, Gu H, Zhang J, Huang et al. Synthesis of an octathienyl-fused phthalocyanine as a donor material for organic solar cells. Dyes and Pigments 2015; 114: 124-128.
6. Polat MP, Yenilmez HY, Koca A, Altındal A, Bayır ZA. Metallophthalocyanines bearing four 3-(pyrrol-1-yl) phenoxy units as photosensitizer for dye-sensitized solar cells. Dyes and Pigments 2018; 156: 267-275.
7. Sevim AM, Çakar S, Özacar M, Gül A. Electrochemical and photovoltaic properties of highly efficient solar cells with cobalt/zinc phthalocyanine sensitizers. Solar Energy 2018; 160: 18-24.

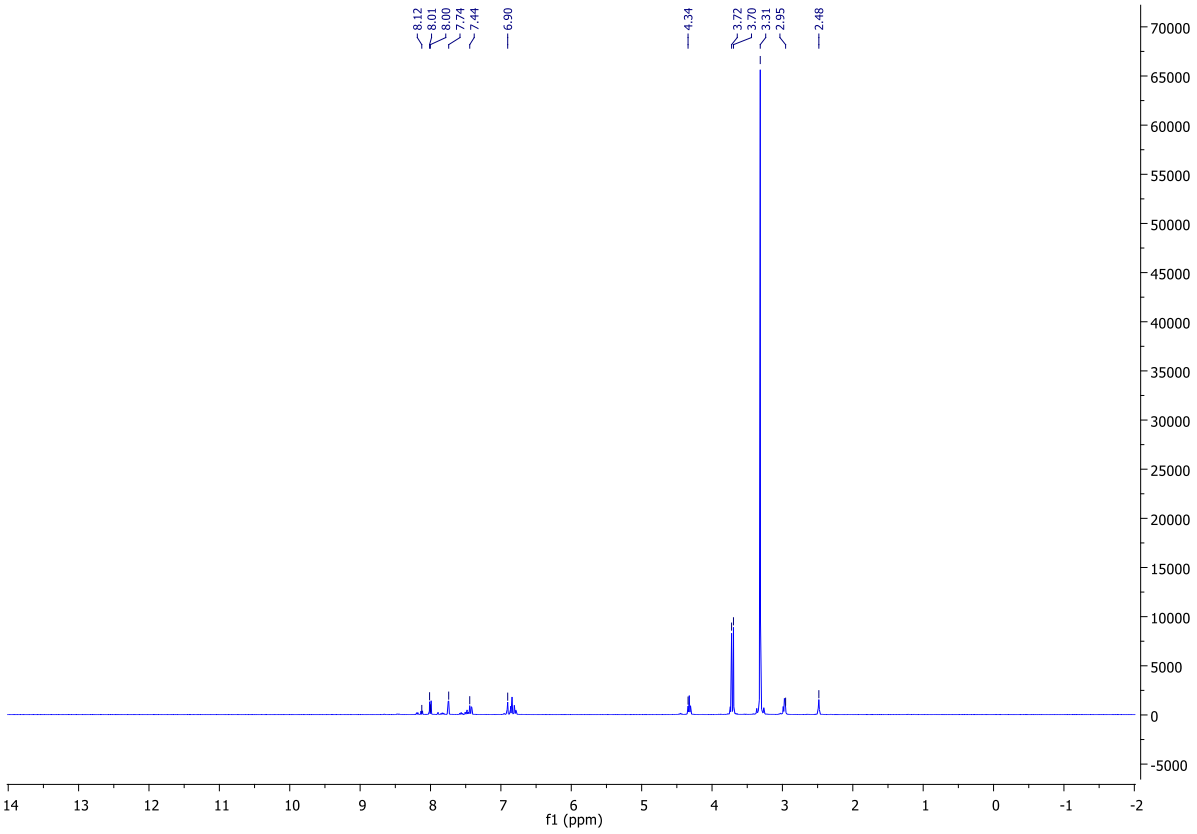

Figure S1. ^{1}H-NMR spectra of compound **3**.

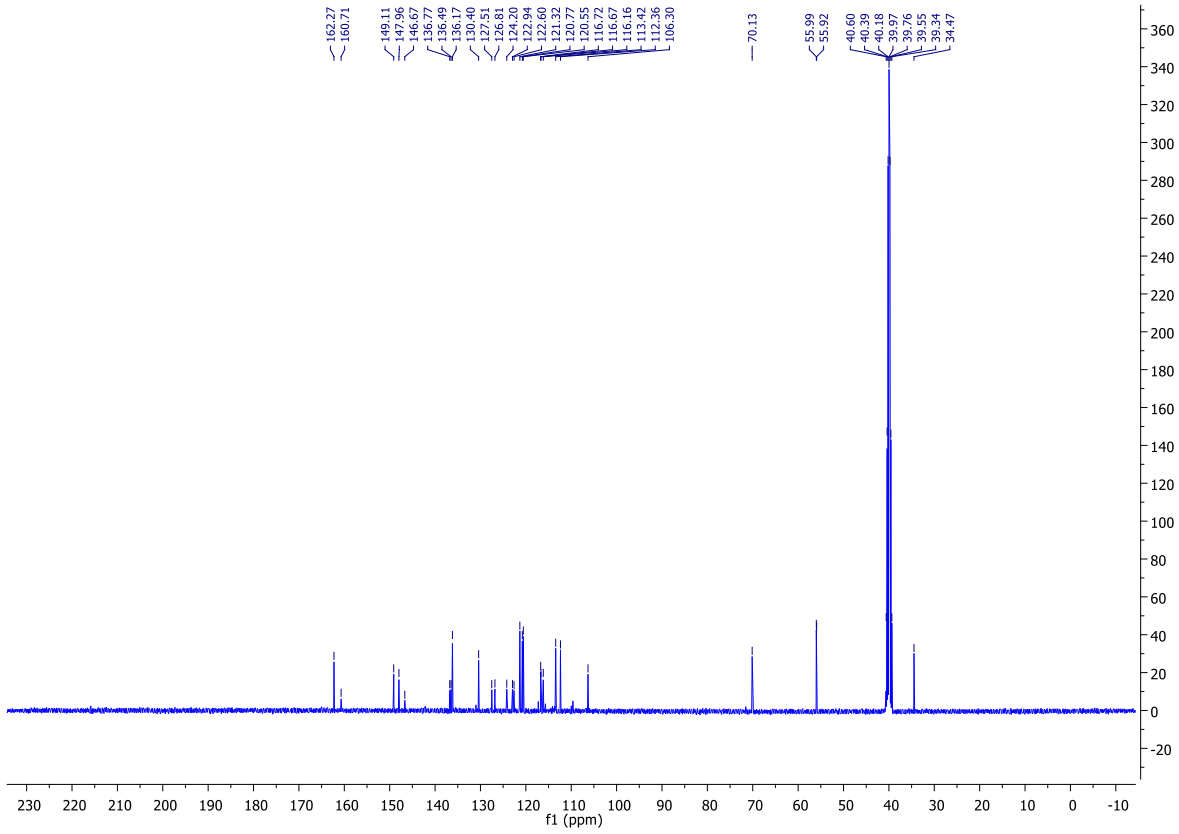

Figure S2. ^{13}C-NMR spectra of compound **3**.

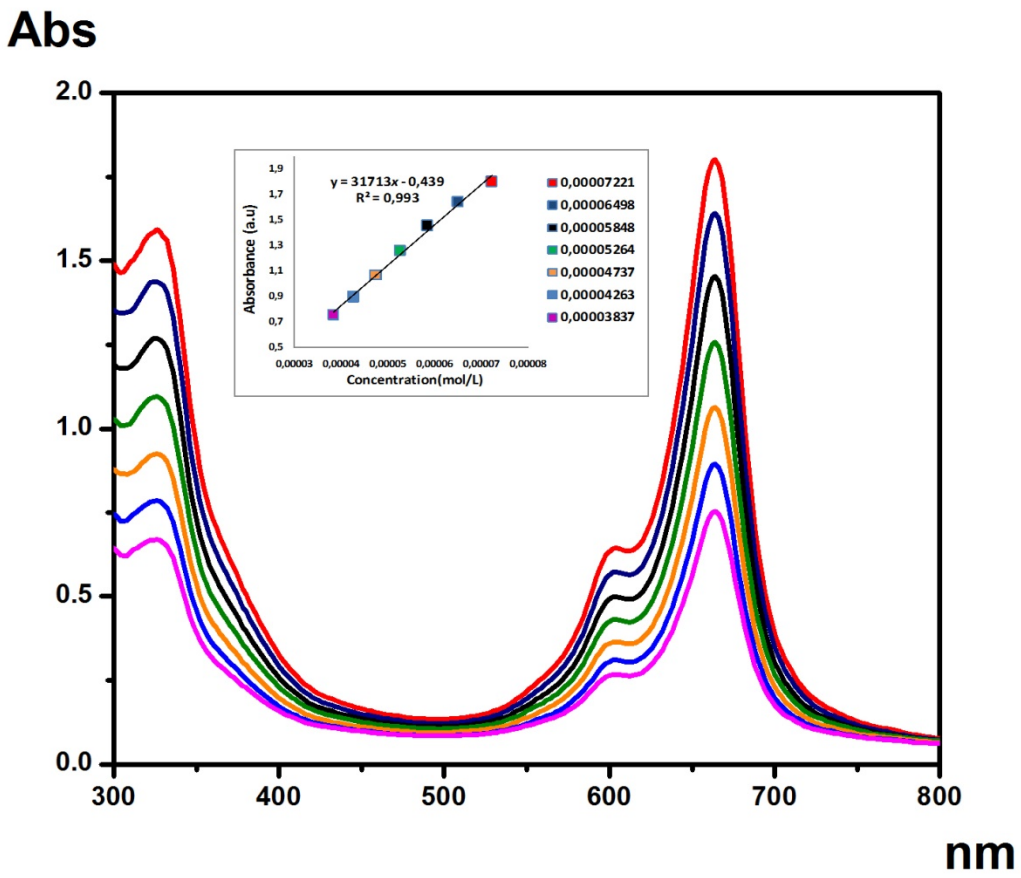

Figure S3. Electronic absorption of compound **5** in different concentrations.

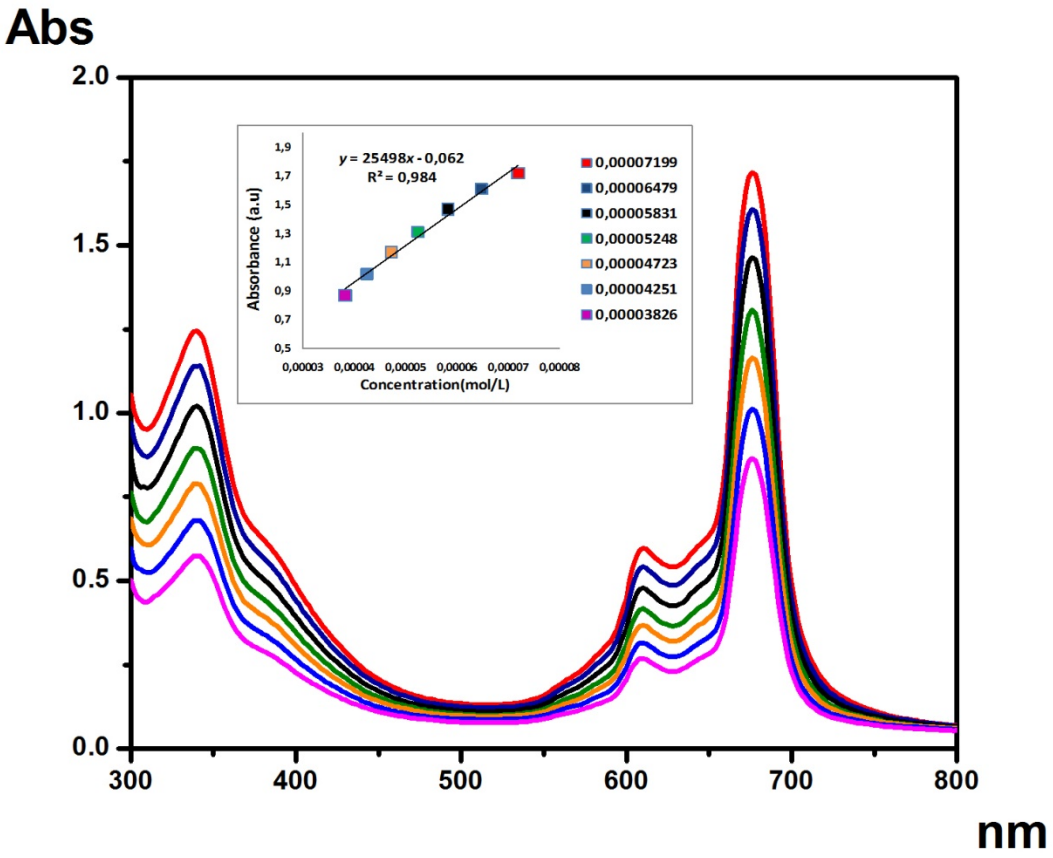

Figure S4. Electronic absorption of compound **6** in different concentrations.

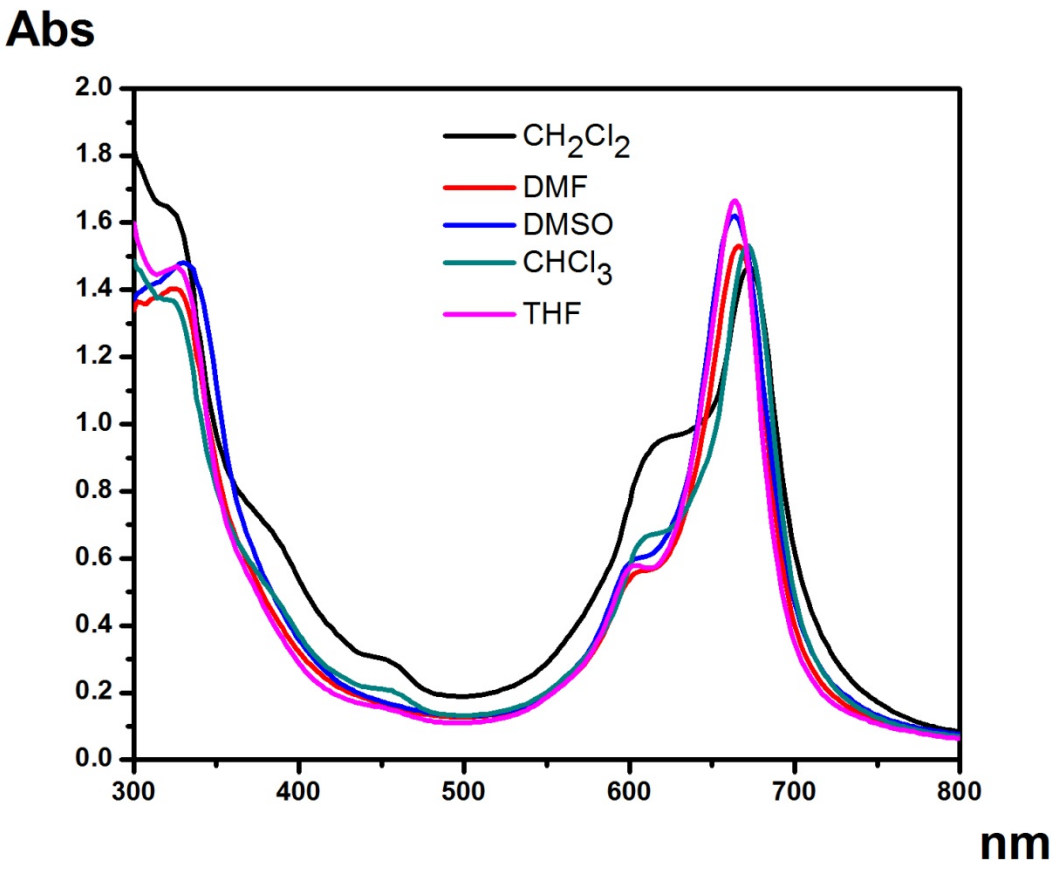

Figure S5. Electronic absorption of compound **5** in different solvents.

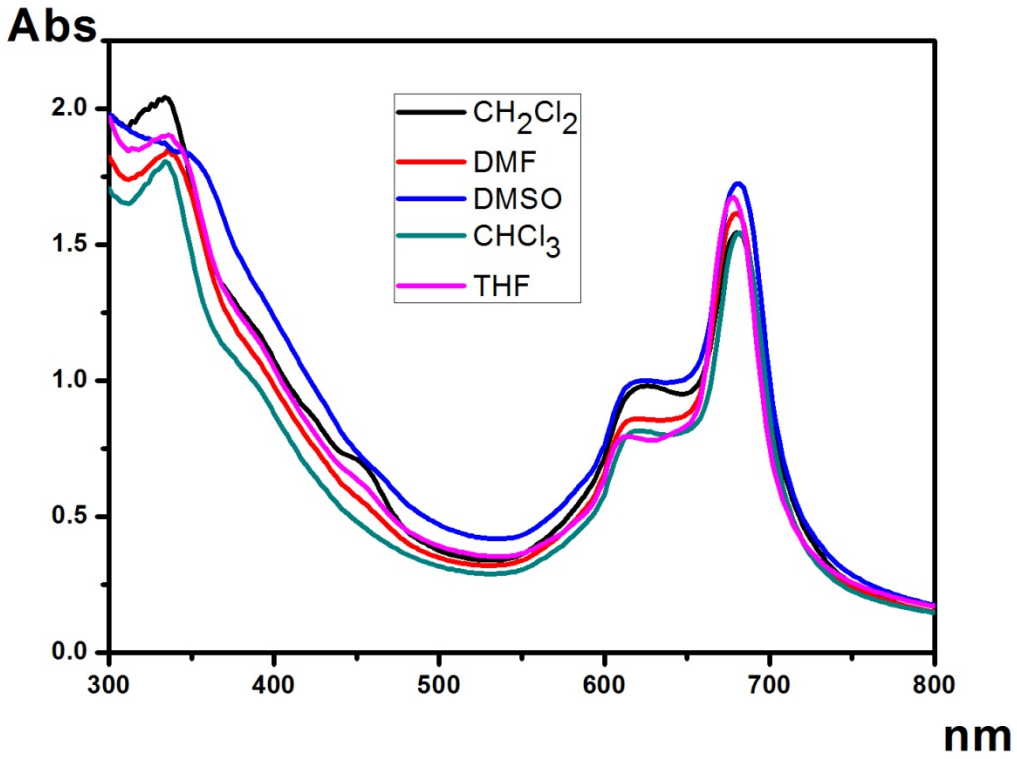

Figure S6. Electronic absorption of compound **6** in different solvents.